Short communication

Elastic modulus and internal friction of SOFC electrolytes at high temperatures under controlled atmospheres

Takuto Kushi[a], Kazuhisa Sato[b], Atsushi Unemoto[b], Shinichi Hashimoto[a], Koji Amezawa[a,*], Tatsuya Kawada[a]

[a] Graduate School of Environmental Studies, Tohoku University, 6-6-01 Aoba, Aramaki, Aoba-ku, Sendai 980-8579, Japan
[b] Institute of Multidisciplinary Research for Advanced Materials, Tohoku University, 2-1-1 Katahira, Aoba-ku, Sendai 980-8577, Japan

ARTICLE INFO

ABSTRACT

Mechanical properties such as Young's modulus, shear modulus, Poisson's ratio and internal friction of conventional electrolyte materials for solid oxide fuel cells, $Zr_{0.85}Y_{0.15}O_{1.93}$ (YSZ), $Zr_{0.82}Sc_{0.18}O_{1.91}$ (ScSZ), $Zr_{0.81}Sc_{0.18}Ce_{0.01}O_{2-\delta}$ (ScCeSZ), $Ce_{0.9}Gd_{0.1}O_{2-\delta}$ (GDC), $La_{0.8}Sr_{0.2}Ga_{0.8}Mg_{0.15}Co_{0.05}O_{3-\delta}$ (LSGMC), $La_{0.8}Sr_{0.2}Ga_{0.8}Mg_{0.2}O_{3-\delta}$ (LSGM), were evaluated by a resonance method at temperatures from room temperature to 1273 K in various oxygen partial pressures. The Young's modulus of GDC gradually decreased with increasing temperature in oxidizing conditions. The Young's moduli of the series of zirconia and lanthanum gallate based materials drastically decreased in an intermediate temperature range and increased slightly with increasing temperature at higher temperatures. The Young's modulus of GDC considerably decreased above 823 K in reducing atmospheres in response to the change of oxygen nonstoichiometry. However, temperature dependences of the Young's moduli of ScCeSZ and LSGMC in reducing atmospheres did not show any significant differences with those in oxidizing atmospheres.

© 2011 Elsevier B.V. All rights reserved.

1. Introduction

There are growing needs for more environmentally friendly and efficient means of energy conversion to fulfill the requests on saving fossil fuels and decreasing the carbon dioxide emission. As such energy conversion devices, solid oxide fuel cells (SOFCs), which can directly convert chemical energy of fuels into electricity, are attracting considerable attentions. SOFCs are now in a demonstrative research stage for their practical use. In Japan for instance, demonstration tests of small-scale stationary SOFCs have been performed since 2007. Consequently it is claimed that improving the durability of SOFCs is particularly important for its commercialization. Mechanical damage is one of the most serious problems that may cause degradation or even destruction of the cell and the stack. In order to determine an appropriate design and operating conditions of SOFCs while ensuring mechanical reliability, it is necessary to understand mechanical properties of SOFC components under fabricating and operating conditions.

Especially, SOFCs operate at high temperatures. Therefore it is important to evaluate the mechanical properties of SOFC components at high temperatures. In addition, during the operation of SOFC, the electrolyte is placed under significant gradient of oxygen potential. Such an oxygen potential gradient in the electrolyte may induce a gradient of defects' concentration. Some oxides used for an SOFC electrolyte, for instance, the fluorite-structured doped CeO_2 and the perovskite-structured Co-doped lanthanum gallate, are known to exhibit oxygen nonstoichiometry changes depending on temperature and oxygen potential [1,2]. The variation in oxygen vacancy concentration may influence mechanical properties. Therefore, it is important to evaluate their mechanical properties in desired temperatures and oxygen partial pressures. Although there exist several reports on the mechanical properties of the typical SOFC electrolytes [3–5], the data at high temperatures [6–8] under controlled atmospheres [9,10] are limited. Thus, further investigation on the mechanical properties at high temperatures under controlled atmospheres is highly required.

In this article, we report the elastic modulus and the internal friction at various temperatures and oxygen partial pressures of the following materials: $Zr_{0.85}Y_{0.15}O_{1.93}$ (YSZ), $Zr_{0.82}Sc_{0.18}O_{1.91}$ (ScSZ), $Zr_{0.81}Sc_{0.18}Ce_{0.01}O_{2-\delta}$ (ScCeSZ), $Ce_{0.9}Gd_{0.1}O_{2-\delta}$ (GDC), $La_{0.8}Sr_{0.2}Ga_{0.8}Mg_{0.15}Co_{0.05}O_{3-\delta}$ (LSGMC), $La_{0.8}Sr_{0.2}Ga_{0.8}Mg_{0.2}O_{3-\delta}$ (LSGM). A resonance method was applied to evaluate the mechanical properties so that measurements could be performed as a function of temperature with one sample. Since all of these materials are expected to used as an SOFC electrolyte, the data obtained in this work will be contribute to the material choice, and determination of its cell designs and operation conditions, leading to the practical use of SOFC.

* Corresponding author. Tel.: +81 22 795 6976; fax: +81 22 795 4067.
E-mail address: amezawa@ee.mech.tohoku.ac.jp (K. Amezawa).

2. Experimental

2.1. Sample preparation

Powder of GDC was prepared by a co-precipitation method. The aqueous solutions of $Ce(NO_3)_3$ and $Gd(NO_3)_3$ were prepared and mixed in an appropriate ratio. Precipitates were obtained by pouring the mixture of the nitrate solutions into oxalic ethanol, filtered and calcined at 1073 K for 3 h in air. Commercial powders of YSZ, ScSZ, ScCeSZ, LSGM and LSGMC were used for the preparation of their sintered compacts.

The powders were hydrostatically pressed at 150 MPa into compacts, and then sintered in air at 1823 K for GDC, at 1623 K for YSZ, and at 1673 K for ScSZ and ScCeSZ. For the resonance measurements, the sintered compacts were cut into rectangles (ca. 8 mm × 1.5 mm × 45 mm), and polished with the diamond paste of 3 μm.

2.2. Sample characterization

Mechanical properties, the Young's modulus, the shear modulus and the internal friction, were investigated using an elastic modulus and an internal friction meter (JE, JG, EG-HT or EGII-HT, Nihon Technoplus Co. Ltd.). JE and JG can perform free hold resonance measurements and EG-HT and EGII-HT can perform cantilever resonance measurements. According to the following equation, Young's modulus and shear modulus were calculated from the resulting resonance frequency and the sample size,

$$E = \frac{4\pi L^4 \rho S}{\alpha^2 I} f_Y^2 \tag{1}$$

$$G = \frac{16L^2 \rho K^2}{\beta} f_S^2 \tag{2}$$

where, E, f_Y, L, α, I, ρ, S, G, f_S, β, and K are the Young's modulus, the flexural resonance frequency, the length of the sample, a constant given by the boundary condition, the moment of inertia, the density of sample, the cross-sectional area, the shear modulus, the torsional resonance frequency, the inertia moment of the drive section, and the adjustment parameter, respectively. The Poisson's ratio was calculated from the values of the Young's modulus and the shear modulus.

In order to control atmospheres, a gas mixing system and an oxygen sensor are additionally attached to the commercial resonance measurement system. Oxygen partial pressure was monitored by the outlet gas stream from the chamber. The atmosphere was controlled by O_2/Ar gas mixtures for high P_{O_2} region and Ar/H_2/H_2O mixtures for low P_{O_2} region. For oxidizing atmosphere, P_{O_2} was fixed as 9.6×10^{-3} or 1.2×10^{-4} bar. For reducing atmosphere, gas mixtures of 1% H_2–0.85% H_2O–98.15% Ar or 99.15% H_2–0.85% H_2O was flowed. P_{O_2} of the above gas mixtures for the reducing atmospheres varies with temperature. For instance, P_{O_2} of 1% H_2–0.85% H_2O–98.15% Ar and 99.15% H_2–0.85% H_2O are 3.1×10^{-19} bar and 3.1×10^{-23} bar at 1073 K, and 3.6×10^{-17} bar and 3.6×10^{-21} bar at 1173 K, respectively.

For the measurements of the mechanical properties, the Young's modulus and shear modulus were first measured at room temperature by using JE and JG. And then, measurements were carried out from room temperature to 1273 K with a 25–50 K interval by using EG-HT or EGII-HT in various oxygen partial pressures. The data obtained by EG-HT or EGII-HT were calibrated by the data at room temperature obtained by JE and JG. The calibration was performed because the free hold resonance measurement has a higher accuracy in absolute value than the cantilever resonance measurement [11]. For ensuring the equilibrium between a sample and the temperature/atmosphere, measurements were repeated until the
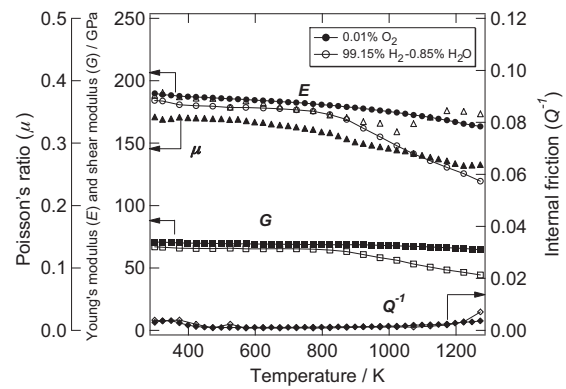
Fig. 1. Young's modulus (●, ○), shear modulus (■, □), Poisson's ratio (▲, △) and internal friction (◆, ◇) of $Ce_{0.9}Gd_{0.1}O_{2-\delta}$ (GDC) in an oxidizing atmosphere of 0.01% O_2 and a reducing atmosphere of 99.15% H_2–0.85% H_2O as functions of temperature. Closed and open symbols represent values in the oxidizing and the reducing atmospheres, respectively.

measured absolute values reached to a constant one while keeping temperature and P_{O_2} around the sample stable.
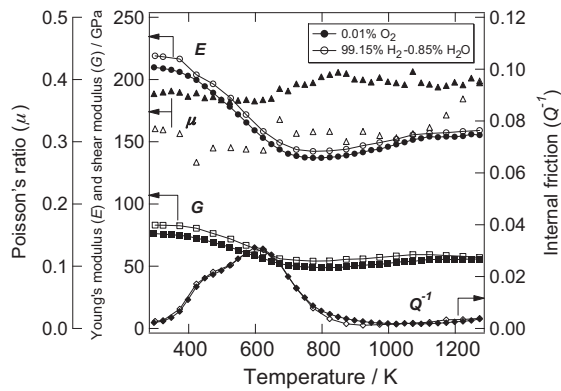
3. Results and discussion

3.1. $(Gd_2O_3)_{0.05}(CeO_2)_{0.9}$ (GDC)

Mechanical properties of GDC in an oxidizing atmosphere of 0.01% O_2 and a reducing atmosphere of 99.15% H_2–0.85% H_2O as functions of temperature are given in Fig. 1. The Young's modulus and the shear modulus in 0.01% O_2 gradually decreased with increasing temperature while the internal friction did not show any apparent changes. Such a gradual temperature dependence of the elastic modulus is typically seen with conventional ceramics and is considered due to decrease in the bonding strength caused by increase in the atomic distance with increasing temperature, i.e., thermal expansion [12,13]. Wachtman et al. reported that the elastic modulus of the conventional ceramics, such as Al_2O_3, MgO, ThO_2, empirically shows the temperature dependence given by the following equation:

$$E = E_0 - BT \exp\left(-\frac{T_0}{T}\right) \tag{3}$$

where E_0 is the modulus at absolute 0 K, and B and T_0 are arbitrary constants [12]. They also suggested that the elastic modulus can be approximated to be proportional to temperature in the temperature range above a few hundred Kelvin because the factor of $\exp(-T_0/T)$ in Eq. (3) approaches to unity at relatively higher temperatures. The proportional factor of the temperature dependence, B, for GDC in 0.01% O_2 was approximately 0.05 GPa K^{-1}, which was in the same order as those reported for conventional ceramics [12,13].

On the other hand, the temperature dependence of the Young's modulus and the shear modulus in the reducing atmosphere was rather different from those in the oxidizing atmosphere. They gradually decreased from room temperature to 823 K, similarly as those in the oxidizing atmosphere, but decreased drastically above 823 K. GDC is known to show the oxygen nonstoichiometry changes at relatively higher temperature in hydrogen reducing conditions, although the oxygen nonstoichiometry is kept almost constant, $\delta = 0.05$, at lower temperature as well as in the oxidizing conditions. For instance, according to the data by Yashiro et al., under the atmosphere of 99.15% H_2–0.85% H_2O, it is calculated that the oxygen nonstoichiometry of GDC starts to change around 873 K ($\delta = 0.05$) and reaches $\delta = 0.64$ at 1273 K [14]. Wang et al. reported the lattice constant of GDC as a function of temperature by using
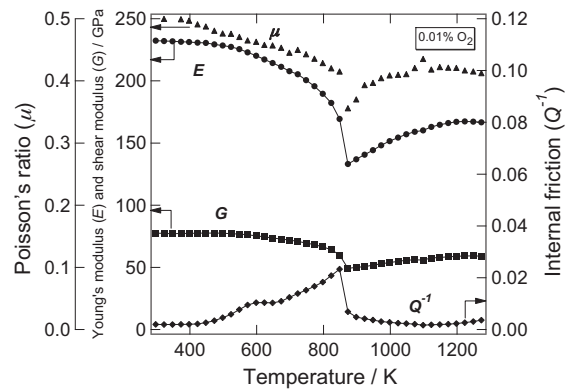
Fig. 2. Young's modulus (●, ○), shear modulus (■, □), Poisson's ratio (▲, △) and internal friction (♦, ◇) of $Zr_{0.85}Y_{0.15}O_{1.93}$ (YSZ) in an oxidizing atmosphere of 0.01% O_2 and a reducing atmosphere of 99.15% H_2–0.85% H_2O as functions of temperature. Closed and open symbols represent values in the oxidizing and the reducing atmospheres, respectively.

Fig. 3. Young's modulus (●), shear modulus (■), Poisson's ratio (▲) and internal friction (♦) of $Zr_{0.82}Sc_{0.18}O_{1.91}$ (ScSZ) in an oxidizing atmosphere of 0.01% O_2 as functions of temperature.

high-temperature XRD. Under the atmosphere of 100% O_2, the lattice constant increases linearly from 5.42 Å to 5.48 Å from room temperature to 1273 K. Under the atmosphere of 98.4% H_2–1.6% H_2O, the lattice constant increases from 5.42 Å to 5.46 Å linearly from room temperature to 873 K, similarly as that under 100% O_2, but increases considerably above 873 K and reaches 5.56 Å at 1273 K [15]. The temperature where the elastic modulus drastically changes seems to agree with the temperature where the oxygen nonstoichiometry changes. Therefore, it can be said that the drastic change of the temperature dependence of the elastic modulus as shown in Fig. 1 is attributed to the oxygen nonstoichiometry changes.

Oxygen nonstoichiometry change in GDC is induced by formation of oxygen vacancies. Therefore once the oxygen nonstoichiometry decreases, the crystal lattice of GDC expands because a part of Ce ions is reduced from tetravalent to trivalent. Such a chemical expansion is supposed to reduce the elastic modulus, as a thermal expansion does. From the discussion above it can be concluded that not only thermal expansion due to temperature change but also chemical expansion due to oxygen nonstoichiometry change influences elastic modulus.

3.2. Zirconia-based materials

Mechanical properties of YSZ in 0.01% O_2 and 99.15% H_2–0.85% H_2O as functions of temperature are given in Fig. 2. The Young's modulus in 0.01% O_2 gradually decreased from 209.8 GPa to 137.1 GPa up to 773 K, although its temperature dependence was rather drastic compared with that of GDC. As temperature further increased, the Young's modulus turned to increase above 773 K and reached to 155.5 GPa at 1273 K. Giraud et al. and Adams et al. reported similar temperature dependences of the Young's modulus [6,7]. Giraud et al. determined the Young's modulus by the impulse excitation technique (IET) in argon atmosphere. In their report, the Young's modulus decreased from 205.8 GPa to 136.5 GPa from room temperature to 823 K, then turned to increase above 823 K, and reached to 156.5 GPa at 1273 K. The absolute value of the Young's modulus was about 1–5 GPa different from our work. This slight difference is considered within experimental error probably caused by the difference of measuring method. In their work, the value was scattered in the temperature range from 423 K to 823 K, while such a scattering was not observed in this work. Comparing from their work, the temperature where the Young's modulus started to increase was about 50 K higher than that in this work, but again such a slight difference could be within experimental error maybe caused by the measuring method. The internal fric-

tion showed two peaks around 423 K and 623 K. These two peaks appeared from around 373 K and disappeared up to around 823 K. As seen in Fig. 2, the internal friction seems to show the peaks when the Young's modulus decreased significantly.

Fig. 3 shows the mechanical properties of ScSZ in 0.01% O_2 as functions of temperature. Mechanical properties of ScCeSZ in 0.01% O_2 and 99.15% H_2–0.85% H_2O as functions of temperature are given in Fig. 4. The mechanical properties of ScSZ and ScCeSZ exhibited similar temperature dependence as those of YSZ, although their changes at the intermediate temperatures were more drastic in ScSZ and ScCeSZ than in YSZ. Sudden changes in the temperature dependence of the elastic modulus appeared at 873 K and 723 K for ScSZ and ScCeSZ, respectively. The internal friction peaks appeared at 598 K and 873 K for ScSZ, and 473 K and 673 K for ScCeSZ, respectively. From the results of ScSZ and ScCeSZ, the drastic decrease of the Young's modulus seems to have a correlation with the internal friction peaks at 873 K for ScSZ and 673 K for ScCeSZ, respectively.

A possible explanation for such sudden changes in the mechanical properties in ScSZ and ScCeSZ is the phase transition. For ScSZ, it is demonstrated that a phase transition from the rhombohedral to the cubic occurs around 873 K [16]. As for ScCeSZ, Yarmolenko et al. reported that the sintering temperature influenced the phase stability. They claimed that the commercial powders from Daiichi Kigenso Kagaku Kogyo Co. Ltd. sintered at 1573 K or above exhibited phase transitions twice, one from the cubic to the rhombohedral
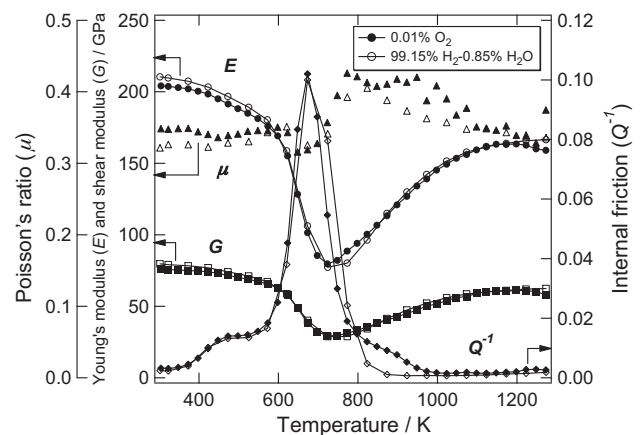
Fig. 4. Young's modulus (●, ○), shear modulus (■, □), Poisson's ratio (▲, △) and internal friction (♦, ◇) of $Zr_{0.81}Sc_{0.18}Ce_{0.01}O_{2-\delta}$ (ScCeSZ) in an oxidizing atmosphere of 0.01% O_2 and a reducing atmosphere of 99.15% H_2–0.85% H_2O as functions of temperature. Closed and open symbols represent values in the oxidizing and the reducing atmospheres, respectively.

and the other from the rhombohedral back to the cubic, when temperature increased from 573 K to 873 K [17]. The phase transition temperatures reported for ScSZ and ScCeSZ in the above work seem to agree well with the temperatures for their changes in mechanical properties displayed in Figs. 3 and 4. Therefore it is concluded that the sudden changes in the mechanical properties in ScSZ and ScCeSZ at the intermediate temperatures are caused by phase transitions.

On the other hand, in YSZ, 8 mol% of yttria doping is believed to stabilize the cubic phase even at lower temperatures [18]. However, the change in the mechanical properties at intermediate temperature was observed also in YSZ, as shown in Fig. 2, although the change in YSZ was more moderate than those in ScSZ and ScCeSZ. There exist some reports claiming that the cubic phase is not stable at lower temperatures and transforms into the tetragonal or the monoclinic phase [19,20]. Considering this, the change in the mechanical properties for YSZ at intermediate temperature might be due to a kind of structural change, even though YSZ did not apparently show a macroscopic phase transition. As displayed in Fig. 2, two internal friction peaks appeared just below the temperature for the sudden change of the mechanical properties. The origin of the internal friction peaks of YSZ was discussed in several literatures [21–24]. Weller et al. assigned the first and the second peaks to the reorientation jumps of the defect pairs $V_o^{\bullet\bullet} - Y'_{Zr}$ representing the elastic and electric dipoles and to the relaxation of oxygen vacancies within a cluster of two or more yttrium ions [21]. Ohta et al. assigned the first and the second peaks to the anisotropic absorption peak due to localized relaxation of oxygen vacancies and to an isotropic oxygen vacancies diffusion relaxation peak [22]. Considering only from the result of YSZ, above factors might influence the mechanical properties as well as the internal friction. However, from the result of ScSZ as shown in Fig. 3, the change of mechanical properties seems to be influenced only by the phase transition. And also from the result of GDC, as shown in Fig. 1, such a kind of change of the mechanical properties have not been seen, which might be also seen if the elastic and electric dipoles or the localized relaxation was the main reason for changing the mechanical properties. GDC is known to have a cubic fluorite structure stably from room temperature to high temperature. Therefore, at the present stage we consider that a partial change in the local coordination, possibly from the tetragonal to the cubic coordination, is the main reason for the drastic decrease of the mechanical properties for YSZ at the intermediate temperature, although the reasons for two peaks of the internal friction were not identified yet.

As described so far, the elastic modulus of the zirconia-based materials drastically decreased at intermediate temperatures while increased at elevated temperatures. This temperature dependency was rather different from one for conventional ceramics, like GDC in 0.01% O$_2$ as shown in Fig. 1. Since the zirconia-based materials are typically used as an SOFC electrolyte material, the data of the elastic modulus are indispensable to evaluate the stress distribution in SOFC. For instance, a decrease of the elastic modulus leads to a decrease of stress for a constant displacement or an increase of displacement for a constant stress. In the case of the zirconia-based materials, estimation of the elastic modulus according to Eq. (3) is not appropriate, and the characteristic temperature dependences of the elastic moduli, which were shown in Figs. 3–5, should be taken into account. This must be important especially when operational margins of SOFC during startup and shutdown are elucidated.

Mechanical properties of YSZ in a reducing atmosphere were measured and the results are shown by open symbols in Fig. 2. As clearly seen, there were no significant differences both in the absolute value as well as the temperature dependence between the results under reducing and oxidizing atmospheres. The oxygen nonstoichiometry of YSZ is known to be almost constant in
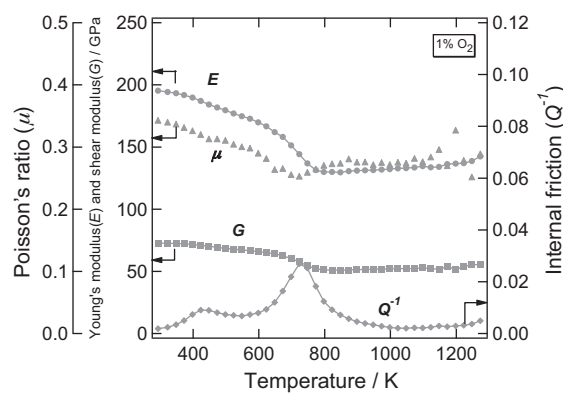

Fig. 5. Young's modulus (●), shear modulus (■), Poisson's ratio (▲) and internal friction (◆) of La$_{0.8}$Sr$_{0.2}$Ga$_{0.8}$Mg$_{0.2}$O$_{3-\delta}$ (LSGM) in an oxidizing atmosphere of 1% O$_2$ as functions of temperature.

the wide ranges of temperature as well as oxygen partial pressure. It is therefore considered that the temperature dependence of the mechanical properties did not vary depending on atmospheric condition. Mechanical properties of ScCeSZ in a reducing atmosphere were also measured, and the results are shown in Fig. 4. There was no significant difference between mechanical properties of ScCeSZ in the oxidizing and the reducing atmospheres. Since ScCeSZ contains Ce ion, the oxygen nonstoichiometry is considered to be changed under reducing conditions as in GDC. However, the mechanical properties did not show apparent difference among employed oxygen partial pressure conditions. A possible explanation for this is that the oxygen nonstoichiometry changes in ScCeSZ were quite smaller than that in GDC. ScCeSZ contains only 1 mol% of Ce, and therefore sufficient changes could not be seen in the mechanical properties in both atmospheric conditions.

4. Lanthanum gallate based materials

Fig. 5 shows the mechanical properties of LSGM in 1% O$_2$ as functions of temperature. The Young's modulus decreased around 773 K, and then turned to increase as temperature increased. In addition, peaks of the internal friction appeared around 423 K and 673 K. Okamura et al. reported the mechanical properties of LSGM measured by a resonance method, although the composition of LSGM was slightly different from one in this work [25]. In their work, mechanical properties of La$_{0.9}$Sr$_{0.1}$Ga$_{0.8}$Mg$_{0.2}$O$_{3-\delta}$ have been determined in the temperature range from room temperature to 1373 K. The temperature dependence of the mechanical properties of LSGM in their work [25] resembled well with those in this work. They also performed high temperature X-ray diffraction measurement. Based on the results, they pointed out that the phase of LSGM was first changed from the pseudo orthorhombic to the pseudo rhombohedral, and then gradually changed from the pseudo rhombohedral to the rhombohedral in the temperature range where the drastic changes of mechanical properties were observed. They, therefore, concluded that the changes of the mechanical properties at the intermediate temperature could be due to the phase transition.

Mechanical properties of LSGMC in oxidizing atmospheres of 1% O$_2$ and 0.01% O$_2$, and a reducing atmosphere of 1% H$_2$–0.85% H$_2$O–98.15% Ar are given in Fig. 6. The Young's modulus decreased around 773 K, and then turned to increase as temperature increased. The internal friction peaks appeared at 423 K and 623 K. Similarly to LSGM, it was reported from high temperature X-ray diffraction measurements that LSGMC exhibits the phase transition from the rhombohedral to the cubic as temperature
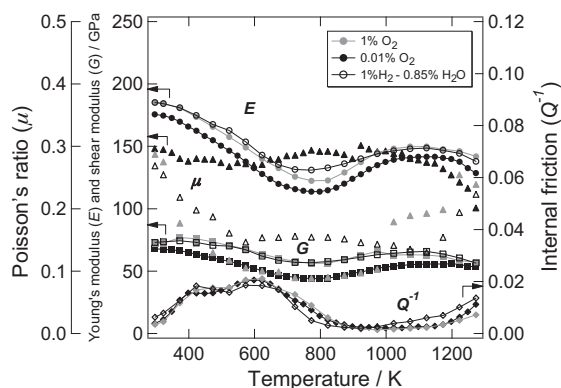
Fig. 6. Young's modulus (●, ●, ○), shear modulus (■, ■, □), Poisson's ratio (▲, ▲, △) and internal friction (◆, ◆, ◇) of $La_{0.8}Sr_{0.2}Ga_{0.8}Mg_{0.15}Co_{0.05}O_{3-\delta}$ (LSGMC) in oxidizing atmospheres of 1% O_2 and 0.01% O_2, and a reducing atmosphere of 1% H_2–0.85% H_2O as functions of temperature. Shaded, closed and open symbols represent values in 1% O_2, 0.01% O_2 and 1% H_2–0.85% H_2O, respectively.

increases [2]. Consequently, it was revealed that the rhombohedral phase is stable at room temperature in air and at temperatures between 573 K and 973 K in $P_{O_2} > 10^{-2}$ bar, while the phase changes to the cubic at temperatures between 573 K and 1173 K in $P_{O_2} > 10^{-2}$ bar. Taking these results into account, the changes of the mechanical properties at intermediate temperatures in LSGMC could be considered due to the phase transition.

From room temperature to 1273 K, temperature dependences of the Young's and the shear moduli were almost similar among employed atmospheric conditions. It is known that LSGMC showed oxygen nonstoichiometry changes at relatively higher temperature even in high oxygen partial pressures, and its amount changes depending on not only temperature but also oxygen partial pressure [2]. However, the mechanical properties did not show sufficient difference among employed oxygen partial pressure conditions. A likely explanation is that the amount of the oxygen nonstoichiometry changes is small and therefore did not considerably influence the mechanical properties.

5. Conclusions

In this work, the Young's modulus and the shear modulus, the Poisson's ratio and the internal friction of the ceria-based, the zirconia-based and the lanthanum gallate-based SOFC electrolyte materials were evaluated in various oxygen partial pressures from room temperature to 1273 K by using a resonance method. It was revealed that the Young's modulus and the shear modulus of GDC showed gradual decrease with increasing temperature under oxidizing atmospheres. On the other hand, the Young's modulus of the YSZ, ScSZ, ScCeSZ, LSGM and LSGMC decreased at intermediate temperatures and turned to increase as temperature further increased. The Young's modulus of GDC decreased drastically from 823 K under reducing atmospheres. Such a drastic change was considered due to its oxygen nonstoichiometry change. However, the

mechanical properties of ScCeSZ and LSGMC had no meaningful difference under both oxidizing and reducing atmospheres.

For the practical uses of the SOFC with a zirconia- or a lanthanum gallate-based electrolyte, the changes in mechanical properties' at intermediate temperatures need to be taken into consideration for determining operating conditions, especially conditions at startup and shutdown. And also, the changes in mechanical properties' at low oxygen partial pressures should be considered for operating condition and cell designs when ceria-based materials are utilized under reducing conditions, for instance, as one component of the cermet anode.

References

[1] S. Wang, H. Inaba, H. Tagawa, M. Dokiya, T. Hashimoto, Solid State Ionics 107 (1998) 73–79.
[2] S. Nakayama, S. Hashimoto, K. Sato, K. Yashiro, K. Amezawa, J. Mizusaki, ECS Trans. 25 (2) (2009) 1701–1708.
[3] A. Selcuk, A. Atkinson, J. Eur. Ceram. Soc. 17 (1997) 1523–1532.
[4] A. Atkinson, A. Selcuk, Solid State Ionics 134 (2000) 59–66.
[5] M. Morales, J.J. Roa, X.G. Capdevila, M. Segarra, S. Pinol, Acta Mater. 58 (2010) 2504–2509.
[6] S. Giraud, J. Canel, J. Eur. Ceram. Soc. 28 (2008) 77–83.
[7] J.W. Adams, R. Ruh, K.S. Mazdiyasni, J. Am. Ceram. Soc. 80 (1997) 903–908.
[8] Y. Du, N.M. Sammes, G.A. Tompsett, D. Zhang, J. Swan, M. Bowden, J. Electrochem. Soc. 150 (1) (2003) A74–A78.
[9] T. Hashida, K. Sato, Y. Takeyama, T. Kawada, J. Mizusaki, ECS Trans. 25 (2) (2009) 1565–1572.
[10] F. Iguchi, Y. Endo, T. Ishida, T. Yokobori, H. Yugami, T. Otake, T. Kawada, J. Mizusaki, Solid State Ionics 176 (2005) 641.
[11] Test method for Young's modulus of metallic materials at elevated temperature, Japanese Industrial Standards, JIS Z2280, 1993.
[12] J.B. Wachtman, W.E. Tefft, D.G. Lam, C.S. Apstein, Phys. Rev. 122 (1961) 1754–1759.
[13] O.L. Anderson, Phys. Rev. 144 (1966) 553–557.
[14] K. Yashiro, S. Onuma, A. Kaimai, Y. Nigara, T. Kawada, J. Mizusaki, K. Kawamura, T. Horita, H. Yokokawa, Solid State Ionics 152–153 (2002) 469–476.
[15] S. Wang, M. Katsuki, T. Hashimoto, M. Dokiya, J. Electrochem. Soc. 150 (2003) A952–A958.
[16] H. Fujimori, M. Yashima, M. Kakihana, M. Yoshimura, J. Appl. Phys. 91 (10) (2002) 6493–6498.
[17] S. Yarmolenko, J. Sankar, N. Bernier, M. Kilmov, J. Kapat, N. Orlovskaya, J. Fuel Cell Sci. Technol. 6 (2009) 021007–21011.
[18] M. Yoshimura, J. Am. Ceram. Soc. 67 (12) (1988) 1950–1955.
[19] M. Yashima, S. Sasaki, M. Kakihana, Solid State Ionics 86–88 (1996) 1131–1149.
[20] B. Butz, P. Kruse, H. Stormer, D. Gerthsen, A. Muller, A. Webber, E. Ivers-Tiffee, Solid State Ionics 177 (2006) 3275–3284.
[21] M. Weller, R. Herzog, M. Kilo, G. Borchardt, S. Weber, S. Scherrer, Solid State Ionics 175 (2004) 409–413.
[22] M. Ohta, K. Kirimoto, K. Nobugai, J.K. Wigmore, T. Miyasato, Physica B 316–317 (2002) 427–429.
[23] A. Lakki, R. Herzog, M. Weller, H. Schubert, C. Reetz, O. Gorke, M. Kilo, G. Borchardt, J. Eur. Ceram. Soc. 20 (2000) 285–296.
[24] M. Weller, B. Damson, A. Lakki, J. Alloys Compd. 310 (2000) 47–53.
[25] T. Okamura, S. Shimizu, M. Mogi, M. Tanimura, K. Furuya, F. Munakata, J. Power Sources 130 (2004) 38–41.